HOKKAIDO UNIVERSITY

Title	Dual-productive photoredox cascade catalyst for solar hydrogen production and methylarene oxidation
Author(s)	Kobayashi, Atsushi
Citation	Catalysis science and technology, (14), 3893-3897 https://doi.org/10.1039/d4cy00544a
Issue Date	2024-07-21
Doc URL	https://hdl.handle.net/2115/95747
Type	journal article
File Information	AK2-PINO-DDSP-system-v2-for-publication(1).pdf

Hokkaido University Collection of Scholarly and Academic Papers : HUSCAP

ARTICLE

Dual-productive photoredox cascade catalyst for solar hydrogen production and methylarene oxidation

Received 00th January 20xx,
Accepted 00th January 20xx

DOI: 10.1039/x0xx00000x

Atsushi Kobayashi*[a]

Solar H_2 production during the transformation of organic compounds is a promising approach to supply both H_2 and organic chemicals necessary for sustainable carbon neutral society. To create such a dual-productive photocatalytic system, we developed a photoredox cascade catalytic (PRCC) system by combining a dual-dye sensitized Pt-TiO_2 photocatalyst (DDSP) and an *N*-hydroxyphthalimide (NHPI) hydrogen atom transfer (HAT) catalyst. DDSP successfully evolved H_2 upon blue-light excitation and simultaneously oxidized NHPI to generate phthalimido-*N*-oxyl radical (PINO•) which produced oxidized methylarenes by the HAT reaction of the benzylic/allylic C-H bond, followed by a radical coupling reaction. The significantly higher activity of DDSP than that of single-dye sensitized analogue (SDSP) suggests that the dual-dye layer acted as an efficent separator to spatially divide the two reaction fields, while separating the electron-hole pairs produced by light absorption with high efficiency.

Introduction

Hydrogen is a key energy material for sustainable carbon neutral society.[1-3] Since the discovery of Honda-Fujishima effect,[4] solar water splitting by semiconductor photocatalyst has been extensively studied as the most promising technique to convert sunlight to hydrogen energy without a negative environmental impact.[5-9] Although water splitting with almost 100% quantum yield was recently achieved by UV-light-driven semiconductor photocatalysts,[10] visible-light-driven photocatalysts still suffer from rapid charge-recombination, undesirable back reactions, and slow kinetics in the water oxidation process.[11-12] Sacrificial reagents as the hole scavenger have been used to promote H_2,[13] but the sacrificial decomposition process replacing water oxidation is generally thermodynamically downhill that cancels out the chemical energy stored during the solar H_2 generation.[14] Concurrent organic synthesis with H_2 production by semiconductor photocatalyst is a promising strategy to overcome these issues, because not only clean energy fuel H_2 but also value-added organic chemicals can be coproduced.[15] Various types of oxidative transformations of organic substrates ranging from alcohol oxidation to cross coupling were reported.[16-19] However, even in such the dual-productive photocatalytic system, the charge-recombination in the semiconductor and undesired back reactions at the photocatalyst surface are still serious issues. Thus, a new strategy to spatially separate not only the electron-hole pair but also the two reaction sites for H_2 production and oxidative transformation of organic substrate is strongly required.

Dye sensitization has widely studied in the fields of solar cell and photocatalysis to efficiently utilize visible spectrum of sunlight.[20-22] Recent developments on photosensitizing dye assembly on semiconductor surface suggest that suitable assembling of photosensitizing dyes and electron mediators to form multiple photoredox cascade structure like the electron transport chain in natural photosynthesis is beneficial in separating electron-hole pair as well as reduction and oxidation sites.[23-31] In this work, we developed a new photoredox cascade catalytic (PRCC, Scheme 1) system by combining dual-dye (**RuCP^6** and **RuP^6**) sensitized Pt-TiO_2 H_2 production

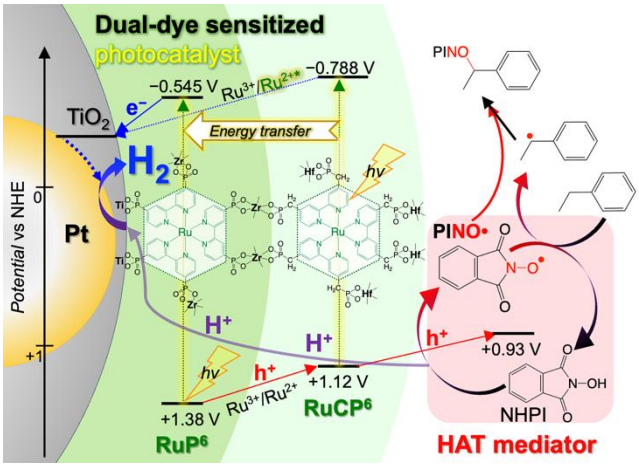

Scheme 1. Schematic energy diagram of PRCC system composed of DDSP and HAT mediator for solar H_2 production and ethylbenzene (EB) oxidation. Possible mechanism: 1) photoexcitation of **RuCP^6** to induce an energy transfer to (or direct photoexcitation of) **RuP^6**,[23] 2) electron injection to Pt-TiO_2, 3) hole transfer from **RuP^6** to NHPI via **RuCP^6** to generate PINO• radical and H^+, 4) HAT by PINO• from benzylic C-H bond to generate NHPI and EB•, and 5) H^+ reduction at Pt-surface[39] and radical coupling to form H_2 and EB-PINO product, respectively. The redox potentials of Ru dyes and NHPI were inferred from the literature.[40-41]

[a] *Department of Chemistry, Faculty of Science, Hokkaido University, Sapporo 060-0810, Japan. E-mail: akoba@sci.hokudai.ac.jp*

Electronic Supplementary Information (ESI) available: Experimental details; Characterization of DDSP; Emission quenching experiment with NHPI; Photocatalytic H_2 evolution by SDSP, etc. See DOI: 10.1039/x0xx00000x

Please do not adjust margins

photocatalyst (DDSP)[27] and *N*-hydroxyphthalimide (NHPI),[32-34] which can act as the hydrogen atom transfer (HAT) mediator to activate benzylic/allylic C–H bonds of various organic substrates. Herein, we demonstrate that the new PRCC system produces H_2 photocatalytically coupled with the benzylic/allylic C-H bond oxidation of methylarenes, and the photocatalytic activity drastically enhanced by the dual-dye layer formation. Although the combination of semiconductor photocatalysts and NHPI has been reported,[35-36] to the best of our knowledge, this is the first dye-sensitized photocatalytic particulate system to achieve both H_2 production and benzylic/allylic C–H bond oxidation with a high apparent quantum yield under blue light irradiation (AQY >3% at 467 nm).

Results and discussion

The DDSP, consisting of Ru(II) dual-dye (**RuCP^6** and **RuP^6**) sensitized Pt-cocatalyst-loaded TiO_2 nanoparticle was synthesized according to our previously reported method with a few modifications (see the Supporting Information for details).[27] Powder X-ray diffraction pattern suggested that the diameter of TiO_2 nanoparticle was 7.5 ± 0.3 nm (Figure S2). UV-vis absorption and X-ray fluorescence spectroscopy revealed that the Pt–TiO_2 nanoparticle surface was fully covered by a dual-dye layer composed of two different Ru(II) dyes and tetravalent cation binders (*i.e.* Hf^{4+}-**RuCP^6**-Zr^{4+}-**RuP^6**), because the estimated footprint of **RuP^6** dye directly anchored on TiO_2 surface was comparable to its molecular size (ca. 0.82 nm^2, Figures S1, S2 and Table S1).

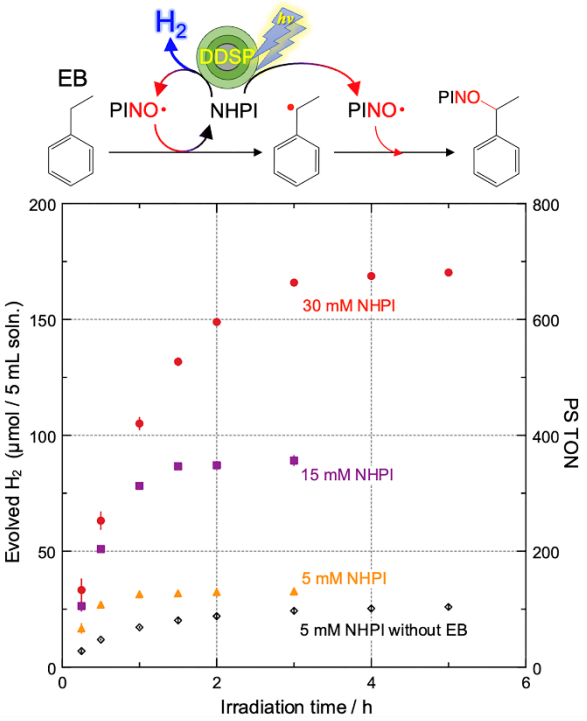

Figure 1. Photocatalytic H_2 evolution by DDSP in the presence of 5-30 mM NHPI, 50 mM pyridine, and 0.1 M ethylbenzene (EB) in CH_3CN under blue-light irradiation (λ = 467 ± 30 nm; 550 mW). The Ru(II) dye concentration was 100 μM for all reactions.

Table 1. Results of photocatalytic H_2 production experiments by DDSP in 50 mM pyridine CH_3CN solution.[a]

Entry	Additives	H_2 (μmol) (0–3 h)	PS TON (0–3 h)	AQY[a] (%) (0–3 h)	*i*AQY (%) (0–0.5 h)
1	5 mM NHPI	24.3 ± 0.10	97.2	0.209	0.612
2	5 mM NHPI +0.1 M EB	32.71 ± 1.5	130.8	0.282	1.395
3	15 mM NHPI +0.1 M EB	89.1 ± 2.0	356.4	0.768	2.63
4	30 mM NHPI +0.1 M EB	165.8 ± 0.10	663.5	1.42	3.27
5	30 mM NHPI +0.1 M EB + 5 mM TBAI	87.7 ±1.39	350.5	0.840	1.00
6	30 mM NHPI +0.1 M *c*-hex	158.3 ± 2.3	633.4	1.36	3.05
7	30 mM NHPI +0.1 M Tol	119.1 ± 0.33	476.2	1.03	2.23
8	30 mM NHPI +0.1 M Tol-d_8	69.1 ± 5.4	276.6	0.596	1.24

a Reaction conditions: [PS] = 100 μM, solution volume = 5 mL; irradiation: λ_{ex} = 467 ± 30 nm, 550 mW. The reaction solution was purged by Ar bubbling for 1 h prior to light irradiation. Values presented as mean ± standard deviation (n ≥ 3). Definitions: AQY = apparent quantum yield, iAQY = AQY in the initial 0.5 h.

We first attempted the photocatalytic H_2 evolution reaction using DDSP in an NHPI solution with 50 mM pyridine as the base to support the proton-coupled oxidation of NHPI (Figure 1). The amount of H_2 evolved, the estimated turn over number per photosensitizer (PS TON), the apparent quantum yield for a total of 3 h (AQY) and the initial 30-min (*i*AQY) reactions are listed in Table 1. H_2 was successfully evolved in the 5 mM NHPI solution (Entry 1), and the estimated PS TON of over 97 after 3 h of irradiation indicates photocatalytic H_2 production coupled with NHPI oxidation to produce the catalytically active phthalimido-*N*-oxyl radical (PINO•). The emission of Ru(II) dyes was hardly quenched by NHPI but effectively quenched by immobilization to TiO_2 (Figure S3). Thus, as discussed in the literature,[23,27,30] the electron injection from photoexcited Ru(II) dyes to TiO_2, followed by hole migration from the inner **RuP^6** to NHPI via the outer **RuCP^6**, is a plausible charge-separation mechanism (Scheme 1). Notably, the *i*AQY doubled upon the addition of 0.1 M ethylbenzene (EB, Entry 2), suggesting that the HAT reaction with EB by PINO• was promoted by the photocatalytic H_2 production of DDSP. Considering that there are 50 equivalents of NHPI (5 mM) per Ru(II) dye (100 μM) in the reaction solution, the estimated PS TON of over 130 indicates all the NHPI molecules were at least twice one-electron oxidized by DDSP. Further enhancement of photocatalytic H_2 evolution (PS TON > 660 and *i*AQY > 3%) was achieved by increasing the NHPI concentration to 30 mM (Entry 4). This *i*AQY value was comparable to that reported for state-of-the-art dye-sensitized photocatalyst for water splitting.[29] In contrast, the PS TON of single-dye sensitized analogue (SDSP) was less than 10% of that for DDSP (Figure 2) and Pt-TiO_2 without any Ru(II) dye hardly evolved H_2 (Figure S4). These results indicate the importance of hole migration in the dual-

This journal is © The Royal Society of Chemistry 20xx

Please do not adjust margins

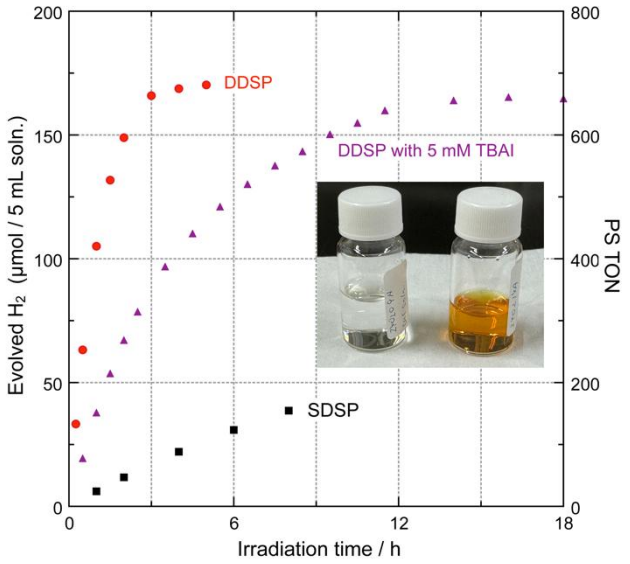

Figure 2. Photocatalytic H_2 evolution by DDSP (red circle) or SDSP (black square) in the presence of 30 mM NHPI, 50 mM pyridine, and 0.1 M ethylbenzene (EB) in CH_3CN under blue-light irradiation (λ = 467 ± 30 nm; 550 mW). Purple triangles show the result in the presence of 5 mM tetrabutylammonium iodide (TBAI). The Ru(II) dye concentration was 100 μM for all reactions. Inset photograph show the reaction supernatants (left) without and (right) with 5 mM TBAI.

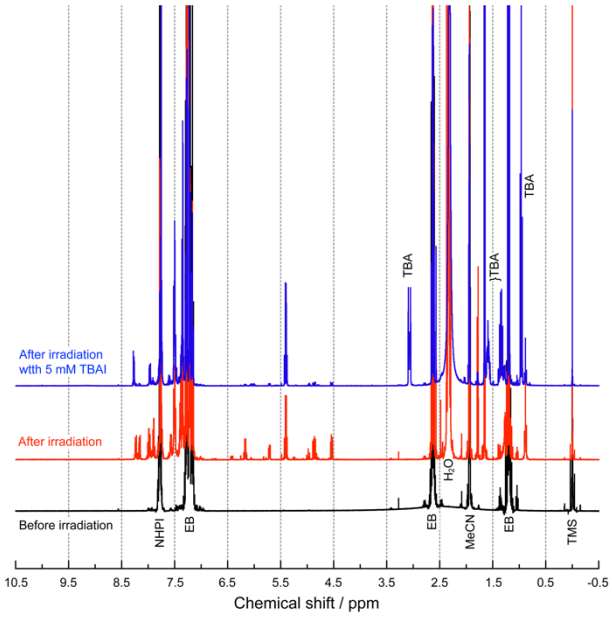

Figure 3. ^{1}H NMR spectra of CD_3CN solution containing 30 mM NHPI, 50 mM pyridine-d^5, and 0.1 M ethylbenzene (black) before and (red) after 5 h light irradiation with DDSP ([Ru] = 100 μM). Top blue lines show the spectra of the solution obtained by the 18 h photocatalytic H_2 evolution reaction in the presence of 5 mM tetrabutylammonium iodide (TBAI).

dye layer for efficient charge-separation as previously reported.[37] The activity of DDSP decreased to 70% by removing 50 mM pyridine (Figure S5), suggesting the important proton accepting role of pyridine during the proton-coupled one-electron oxidation of NHPI. In the ^{1}H NMR spectrum of the reaction supernatant (Figures 3, S6 and S7), several new peaks are observed in the 4.5–6.5 ppm region that were not present before irradiation, suggesting the HAT reaction with PINO•. The intense quartet signal at 5.38 ppm suggests that radical coupling products between the H-atom abstracted EB• species and PINO• (EB-PINO) were photocatalytically produced. H_2 production was almost terminated after 3h of irradiation, presumably because all the NHPI molecules were consumed, as suggested by the disappearance of UV absorption edge of NHPI at approximately 400 nm (Figure S8(a)) and further extension of the photocatalytic H_2 production by increasing the NHPI concentration from 30 to 100 mM (Figure S9). The other signals in the 4.5–6.5 ppm region can be assigned to the byproducts formed between PINO• and the radical resonant hybrids of EB• (Scheme S1). The overall feature of this spectrum was hardly changed during the photocatalytic H_2 production for the increasing each newly appeared signal intensity (Figure S10), suggesting several by-products photocatalytically and simultaneously generated with the main product, EB-PINO. Notably, such byproduct formation was effectively suppressed by addition of 5 mM tetrabutylammonium iodide (TBAI) as the source of the radical trap, I_2 (Figures 3, S6 and S11).[38] Although the H_2 evolution activity in this condition was lower than that without TBAI because of the light shielding effect of oxidatively generated I_2 and I_3^- species (Entry 5 and Figure 2), the H_2 evolved amount and PS TON after 18h irradiation (164 μmol and PS TON ~ 660) were almost comparable to those without TBAI. The intensity ratio of the terminal methyl proton signal of TBA^+ to the characteristic quartet signal of EB-PINO in the ^{1}H NMR spectrum (2.81: 1, Figure S11) suggests that the final concentration of EB-PINO is 21.7 mM. Considering that the expected concentration of the two-electron oxidized species based on the PS TON and the PS concentration was 33 mM, two of the three PINO• were successfully converted to EB-PINO.

Photocatalytic H_2 evolution in the presence of the other substrates, cyclohexene (*c*-hex) and toluene (Tol), was conducted (Figure 4) to evaluate the versatility of the PRCC system. The evolved H_2 amount in the *c*-hex solution was comparable to that in EB (Entry 6), whereas it decreased to approximately 70% in the Tol solution (Entry 7). This difference could be due to instability of the radical species generated by the HAT reaction with PINO•.[36] Notably, the photocatalytic H_2 production activity was significantly reduced by replacing Tol with deuterated toluene (Tol-d^8, Entry 8), whereas such a decrease was hardly observed when replacing the base and solvent with deuterated ones (Figure S12). Thus, this isotope effect provides direct evidence of the HAT reaction of PINO• with the benzylic/allylic C–H bonds of these substrates. Significant changes in ^{1}H NMR spectra were also observed in these reactions (Figures S13-S16), the HAT reaction by PINO• with these substrates occurring to form radical coupling products. Notably, a singlet signal at 10.0 ppm was observed in the supernatant containing Tol (Figure S16), suggesting the formation of benzaldehyde. Similar to the case of EB solution, the absorption edge of NHPI at approximately 400 nm was significantly weakened after the reaction (Figures S8(b) and S8(c)). Considering that the estimated PS TONs in these reactions were above 300, most of the NHPI were converted to radical coupling products during photocatalytic H_2 evolution by DDSP.

Please do not adjust margins

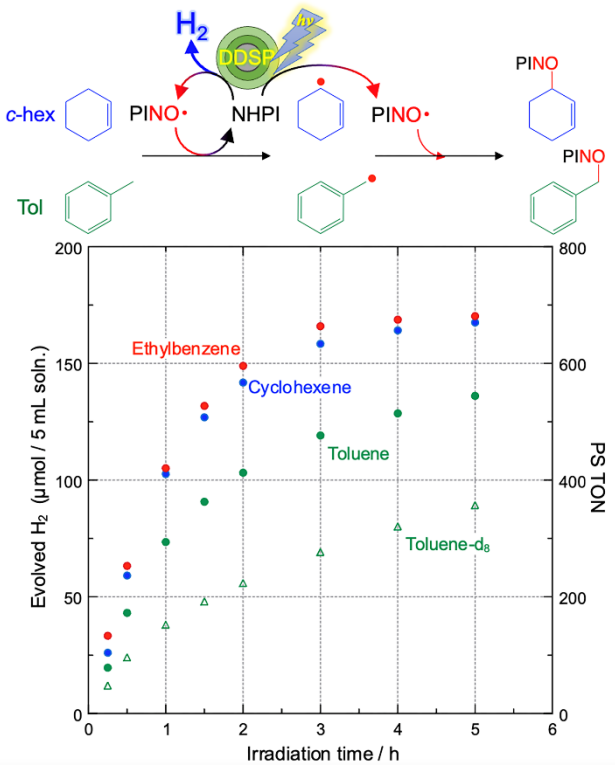

Figure 4. Photocatalytic H_2 evolution by DDSP in the presence of 30 mM NHPI, 50 mM pyridine, and 0.1 M substrates (red: EB, blue: c-hex, green circle: Tol, and green triangle: Tol-d_8) in CH_3CN under blue-light irradiation (λ = 467 ± 30 nm; 550 mW). The Ru(II) dye concentration was 100 μM for all reactions.

Conclusions

This study demonstrates a dual productive photocatalytic reaction involving H_2 evolution by DDSP and NHPI-mediated oxidation of the benzylic/allylic C-H bonds of simple methylarene. The plausible reaction mechanism is as follows; DDSP photocatalytically oxidized NHPI under blue light irradiation to generate H_2 and catalytically active PINO• radical as the reduced and oxidized products, respectively. The HAT reaction of PINO• with benzylic/allylic C-H bonds of methylarenes successfully regenerated NHPI and co-produced radical species of methylarenes. The final radical coupling products were formed by the reaction between the hydrogen-atom abstracted methylarene and PINO• that was reproduced by photocatalytic cycle of DDSP. Although coproduction of H_2 with oxidative transformation of organic chemicals by semiconductor photocatalysts has been extensively studied so far,[15] the suppressing undesired back reaction at photocatalyst surface is still challenging. The significantly higher activity of DDSP than that of SDSP indicates the dual-dye layer on Pt-TiO_2 nanoparticle surface plays the key role in both the charge-separation and suppressing the backward reactions. In other words, the charge-separation after light absorption was facilitated by the photoredox cascade structure built into the dual-dye layer structure (Scheme 1). Further, the thick dual-dye layer spatially divides H_2 production and NHPI oxidation sites into the inner and outer surface of the dual-dye layer, suppressing the backward reactions. We believe that these findings may open a new avenue for efficient coproduction photocatalytic systems for clean energy H_2 and value-added organic chemicals.

Conflicts of interest

There are no conflicts to declare.

Acknowledgements

The author deeply thanks Prof. K. Sada and Dr. Y. Shimizu (Hokkaido University) for their valuable supports and helpful discussions. This study was supported by the ENEOS Hydrogen Trust Fund, the Casio Science Promotion Foundation, the Iwatani Naoji Foundation, and JSPS KAKENHI (grant numbers 23H01969 and 22K19039).

Notes and references

1 S. Chen, T. Takata, K. Domen, *Nat. Rev. Mater.*, 2017, **2**, 17050.
2 F. Dawood, M. Anda, G. M. Shafiullah, *Int. J. Hydrogen Energy*, 2020, **45**, 3847.
3 M. Yue, H. Lambert, E, Pahon, R. Roche, S. Jemei, D. Hissel, *Renewable & Sustainable Energy Rev.*, 2021, **146**, 111180.
4 A. Fujishima, K. Honda, *Nature*, 1972, **238**, 37.
5 A. Kudo, Y. Miseki, *Chem. Soc. Rev.*, 2009, **38**, 253–278.
6 K. Maeda, *ACS Catal.*, 2013, **3**, 1486.
7 J. H. Kim, D. Hansora, P. Sharma, K. -W. Jang, L. S. Lee, *Chem. Soc. Rev.*, 2019, **48**, 1908.
8 Q. Wang, K. Domen, *Chem. Rev.*, 2020, **120**, 919.
9 X. Fang, S. Kalathil, E. Reisner, *Chem. Soc. Rev.*, 2020, **49**, 4926.
10 T. Takata, J. Jiang, Y. Sakata, M. Nakabayashi, N. Shibata, V. Nandal, K. Seki, T. Hisatomi, K. Domen, *Nature*, 2020, **581**, 411.
11 L. Zhang, J. Zhang, H. Yu, J. Yu, *Adv. Mater.*, 2022, **34**, 2107668.
12 Y. Wang, H. Suzuki, J. Xie, O. Tomita, D. J. Martin, M. Higashi, D. Kong, R. Abe, J. Tang, *Chem. Rev.*, 2018, **118**, 5201.
13 Y. Pellegrin, F. Odobel, *C, R, Chimie*, 2017, **20**, 283.
14 J. Schneider, D. W. Bahnemann, *J. Phys. Chem. Lett.*, 2013, **4**, 3479.
15 M.-Y. Qi, M. Conte, M. Anpo, Z.-R. Tang, Y.-J. Xu, *Chem. Rev.*, 2021, **121**, 13051.
16 L.-M. Zhao, Q.-Y. Meng, X.-B. Fan, C. Ye, X.-B. Li, B. Chen, V. Ramamurthy, C.-H. Tung, L.-Z. Wu, *Angew. Chem. Int. Ed.*, 2017, **56**, 3020.
17 H. Zhang, S. Xie, J. Cheng , J. Hu, X. Wu, Q. Zhang, Y. Wang, *Chem. Commun.*, 2020, **56**, 1776.
18 A. Yamamoto, T. Ohara, H. Yoshida, *Catal. Sci. Technol.*, 2018, **8**, 2046.
19 L. Li, S. Fan, X. Mu, Z. Mi, C.-J. Li, *J. Am. Chem. Soc.* 2014, **136**, 7793.
20 B. O'Regan, M. Grätzel, *Nature* 1991, **353**, 737.
21 A. Mishra, M. K. R. Fischer, P. Bäuerle, *Angew. Chem. Int. Ed.* 2009, **48**, 2474.
22 H. Park, Y. Park, W. Kim, W. Choi, *J. Photochem. Photobiol. C*, 2013, **15**, 1.
23 K. Hanson, D. A. Torelli, A. K. Vannucci, M. K. Brennaman, H. Luo, L. Alibabaei, W. Song, D. L. Ashford, M. R. Norris, C. R. K. Glasson, J. J. Concepcion, T. J. Meyer, *Angew. Chem. Int. Ed.* 2012, **51**, 12782.
24 B. H. Farnum, K.-R. Wee, T. J. Meyer, *Nat. Chem.*, 2016, **8**, 845.
25 J. C. Wang, S. P. Hill, T. Dilbeck, O. O. Ogunsolu, T. Banerjee, K. Hanson, *Chem. Soc. Rev.* 2018, **47**, 104.

This journal is © The Royal Society of Chemistry 20xx

Please do not adjust margins

Please do not adjust margins

26 R. N. Sampaio, L. Troian-Gautier, G. J. Meyer, *Angew. Chem. Int. Ed.*, 2018, **57**, 15390.
27 N. Yoshimura, A. Kobayashi, M. Yoshida, M. Kato, *Chem. Eur. J.*, 2020, **26**, 16939.
28 S. Li, S. Kim, A. H. Davis, J. Zhuang, E. W. Shuler, D. Willinger, J.-J. Lee, W. Zheng, B. D. Sherman, C. G. Yoo, G. Leem, *ACS Catal.*, 2021, **11**, 3771.
29 S. Nishioka, K. Hojo, L. Xiao, T. Gao, Y. Miseki, S. Yasuda, T. Yokoi, K. Sayama, T. E. Mallouk, K. Maeda, *Sci. Adv.*, 2022, **8**, eadc9115.
30 A. Kobayashi, *Angew. Chem. Int. Ed.* 2023, **62**, e202313014.
31 A. Arcidiacono, B. Hanks, K. Hanson, *ACS Appl. Opt. Mater.* 2023, **1**, 1156.
32 F. Recupero, C. Punta, *Chem. Rev.* 2007, **107**, 3800.
33 E. J. Horn, B. R. Rosen, Y. Chen, J. Tang, K. Chen, M. D. Eastgate, P. S. Baram, *Nature*, 2016, **533**, 77.
34 J. E. Nutting, M. Rafiee, S. S. Stahl, *Chem. Rev.*, 2018, **118**, 4834.
35 L. Melone, P. Franchi, M. Lucarini, C. Punta, *Adv. Synth. Catal.*, 2013, **355**, 3210.
36 G. Zhao, B. Hu, G. W. Busser, B. Peng, M. Muhler, *ChemSusChem*, 2019, **12**, 2795.
37 N. Yoshimura, M. Yoshida, A. Kobayashi, *J. Am. Chem. Soc.* 2023, **145**, 6035.
38 M. Rafiee, F. Wang, D. P. Hruskewycz, S. S. Stahl, *J. Am. Chem. Soc.*, 2018, **140**, 22.
39 E. D. Fakhrutdinova, O. A. Reutova, T. A. Bugrova, I. Yu. Ovsyuk, L. S. Kibis, O. A. Stonkus, D. B. Vasilchenko, O. V. Vodyankina, V. A. Svetlychnyi, *Trans. Tianjin Univ.*, 2024, **30**, 198; S. Du, J. Lian, F. Zhang, *Trans. Tianjin Univ.*, 2022, **28**, 33.
40 M. R. Norris, J. J. Concepcion, C. R. K. Glasson, Z. Fang, A. M. Lapides, D. L. Ashford, J. L. Templeton, T. J. Meyer, *Inorg. Chem.*, 2013, **52**, 12492.
41 E. Baciocchi, M. Bietti, C. D'Alfonso, O. Lanzalunga, A, Lapi, M. Salamone, *Org. Biomol. Chem.*, 2011, **9**, 4085.

This journal is © The Royal Society of Chemistry 20xx

Please do not adjust margins